

# Luminescence quenching in supramolecular assemblies of quantum dots and bipyridinium dications†

Benoît Gadenne,<sup>a</sup> Ibrahim Yildiz,<sup>b</sup> Matteo Amelia,<sup>a</sup> Flavio Ciesa,<sup>c</sup> Andrea Secchi,<sup>c</sup> Arturo Arduini,<sup>c</sup> Alberto Credi<sup>\*a</sup> and Francisco M. Raymo<sup>\*b</sup>

Received 2nd January 2008, Accepted 18th February 2008

First published as an Advance Article on the web 6th March 2008

DOI: 10.1039/b720038b

We have investigated the ability of two bipyridinium dications, with either octyl or decyl groups on their nitrogen atoms, to quench the luminescence of CdSe–ZnS core–shell quantum dots coated by either tri-*n*-octylphosphine oxide or a tris(phenylureido)calix[6]arene. Our studies demonstrate that both bipyridinium dications adsorb on the surface of the quantum dots with association constants ranging from  $10^4$  to  $10^7$  M<sup>-1</sup> and quench the luminescence of the inorganic nanoparticles with rate constants ranging from  $10^8$  to  $10^9$  s<sup>-1</sup>. The association constants of these supramolecular assemblies vary significantly with the counterions of the bipyridinium dications and the ligands on the nanoparticle surface. Their quenching rate constants vary with the length of the alkyl chains appended to the bipyridinium core and, once again, the ligands on the nanoparticle surface. Furthermore, our studies show that the addition of a calix[6]arene able to compete with the quantum dots for the bipyridinium quenchers restores the original luminescence intensity of the nanoparticles. Indeed, the supramolecular association of the calix[6]arene with the bipyridinium dication removes the quencher from the nanoparticle surface and, hence, is transduced into a luminescent enhancement.

## Introduction

Semiconductor quantum dots (QDs) are inorganic particles with nanoscaled diameters and outstanding photophysical properties.<sup>1–5</sup> Their spectroscopic signature can be manipulated with fine adjustments in elemental composition and physical dimensions to afford luminescent probes with tunable emissive behavior. Indeed, the modularity of these inorganic nanostructures coupled to intrinsically high absorption cross sections, outstanding photobleaching resistances and long luminescence lifetimes are encouraging their use in biomedical imaging and sensing applications as an alternative to conventional organic fluorophores.<sup>6–12</sup> Specifically, protocols to signal target analytes with luminescent QDs are starting to be developed on the basis of electron and energy transfer processes.<sup>13,14</sup> In fact, fundamental investigations have demonstrated that these inorganic nanostructures can exchange electrons with complementary organic partners upon excitation with a concomitant luminescence quenching.<sup>15–20</sup> In particular, we have exploited the ability of CdSe–ZnS core–shell QDs to inject electrons into bipyridinium dications to develop photochromic materials<sup>18a</sup> and probe protein–ligand interactions.<sup>18d</sup> These strategies are based on the

adsorption of appropriate bipyridinium dications on the surface of the inorganic nanoparticles in the ground state and on the exchange of electrons between them in the excited state. In order to elucidate further the fundamental factors governing these processes and broaden the array of basic building blocks available for the implementation of these strategies, we have prepared QDs coated with either tri-*n*-octylphosphine oxide (TOPO) or a tris(phenylureido)calix[6]arene (**3** in Fig. 1) and investigated

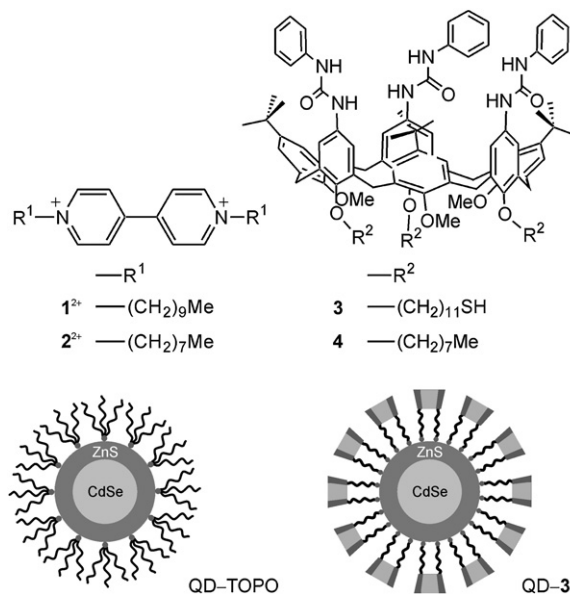


**Fig. 1** The bipyridinium dications **1<sup>2+</sup>** and **2<sup>2+</sup>**, the calixarenes **3** and **4** and schematic representations of QD-TOPO and QD-3 (the schematic representations are not to scale).

<sup>a</sup>Dipartimento di Chimica "G. Ciamician", Università di Bologna, via Selmi 2, 40126 Bologna, Italy. E-mail: alberto.credi@unibo.it

<sup>b</sup>Center for Supramolecular Science, Department of Chemistry, University of Miami, 1301 Memorial Drive, Coral Gables, FL 33146-0431, USA. E-mail: fraymo@miami.edu

<sup>c</sup>Dipartimento di Chimica Organica e Industriale, Università di Parma, via G.P. Usberti 17/a, 43100 Parma, Italy

† Electronic supplementary information (ESI) available: Calculation of the size of the inorganic nanocrystals; DLS experiments; <sup>1</sup>H NMR and ESIMS spectra of **3**; analysis of the Stern–Volmer plots. See DOI: 10.1039/b720038b

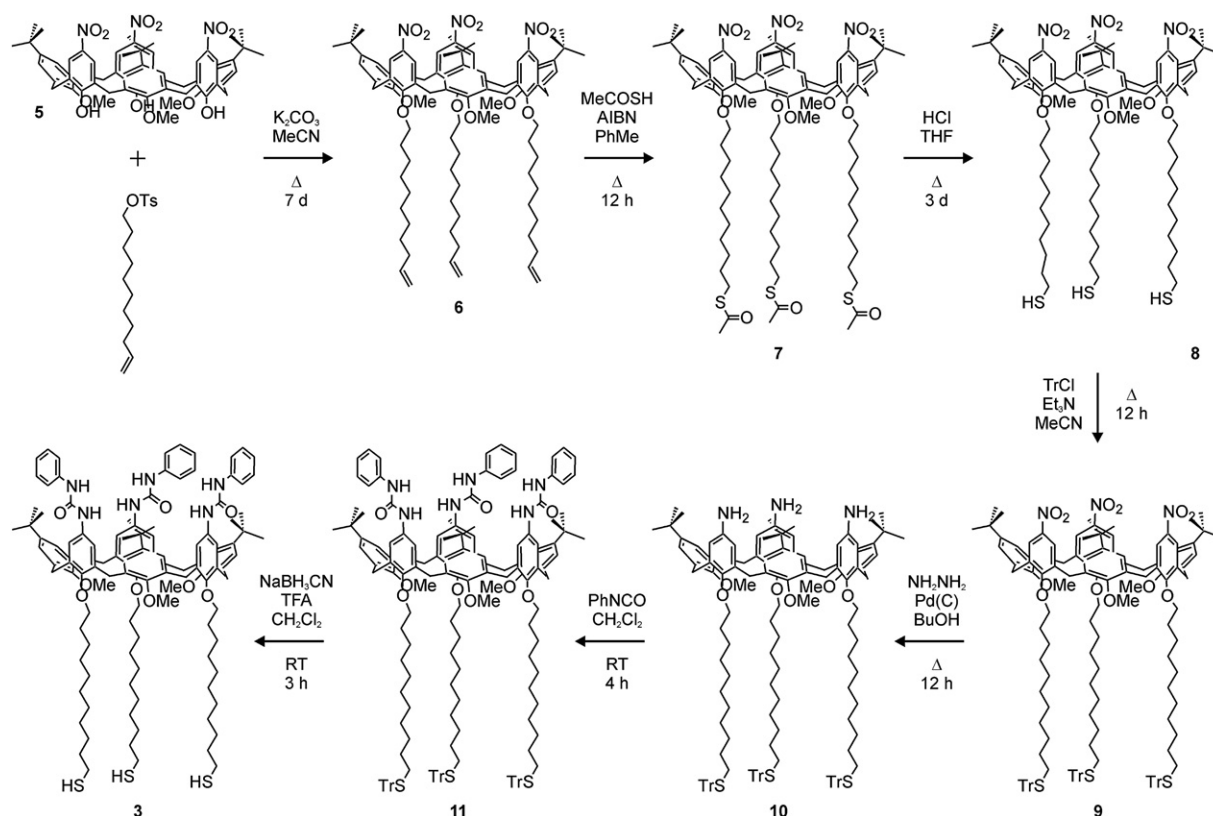


Fig. 2 Synthesis of the calixarene 3.

the interactions of the resulting assemblies QD–TOPO and QD–3 with the bipyridinium dication  $1^{2+}$  and  $2^{2+}$  (Fig. 1).

## Results and discussion

### Synthesis and characterization

**QDs.** We have synthesized QD–TOPO according to established literature procedures.<sup>21,22</sup> Specifically, we have reacted CdO and Se at high temperature in the presence of TOPO and treated the resulting nanoparticles with  $\text{Et}_2\text{Zn}$  and hexamethyldisilathiane to generate QD–TOPO. We have then heated a dispersion of QD–TOPO and **3** in  $\text{CHCl}_3$  under reflux for one day and isolated QD–3 after reiterative precipitation, centrifugation and filtration steps.

The diameter of the CdSe core and that of the CdSe–ZnS core–shell assembly have been estimated to be 2.8 and 5.3 nm, respectively, from absorption data and stoichiometric considerations.<sup>‡</sup> The hydrodynamic diameters of QD–TOPO and QD–3 have been determined by dynamic light scattering (DLS) experiments. QD–TOPO particles exhibit a diameter of  $9 \pm 1$  nm, *i.e.*, much larger than the 5.3 nm calculated for the inorganic core–shell assembly. However, both the contribution of the ligand shell and solvation sphere effects need to be taken into account. Recent experiments have shown that the apparent thickness of the TOPO shell ranges from 1.3 to 2 nm.<sup>23</sup> Therefore, the value of the diameter measured by DLS is in full agreement with the

calculated size of the inorganic nanocrystal. Calixarene-coated QD–3 have been found to exhibit a hydrodynamic diameter of  $16 \pm 3$  nm, *i.e.*, considerably larger than that observed for QD–TOPO. This difference can hardly be accounted for by the larger size of **3** compared to TOPO; in fact, the high polydispersion index ( $>0.7$ ) suggests that nanoparticle aggregates may be present.

**Bipyridinium derivatives.** We have synthesized compounds  $1^{2+}$  and  $2^{2+}$  according to established literature procedures.<sup>24,25</sup> In particular, we have reacted 4,4′-bipyridine with an excess of either decylbromide or octylbromide and then exchanged the bromide counterions of the resulting dication with either hexafluorophosphate or chloride anions to generate  $1 \cdot 2\text{Cl}$ ,  $1 \cdot 2\text{PF}_6$  and  $2 \cdot 2\text{PF}_6$ .

**Calixarene derivative.** We have prepared **3** in six steps (Fig. 2) starting from known precursors.<sup>26,27</sup> In particular, we have alkylated the calixarene **5** with toluene-4-sulfonic acid undec-10-enyl ester, under the assistance of  $\text{K}_2\text{CO}_3$ , and reacted the resulting compound **6** with thioacetic acid, in the presence of AIBN. After the acid hydrolysis of the thioester groups of **7**, we have alkylated the thiol groups of **8** with trityl chloride, under the assistance of  $\text{Et}_3\text{N}$ . Then, we have reduced the nitro groups of **9** with hydrazine, in the presence of catalytic amounts Pd(C), and reacted the amino groups of **10** with phenylisocyanate. Finally, we have removed the trityl groups of **11** with  $\text{NaBH}_3\text{CN}$  and TFA to afford the target molecule **3**.<sup>§</sup>

<sup>‡</sup> The determination of the core and core–shell diameters is discussed in the ESI.<sup>†</sup>

<sup>§</sup> The  $^1\text{H}$  NMR and ESIMS spectra of **3** are reported in the ESI.<sup>†</sup>

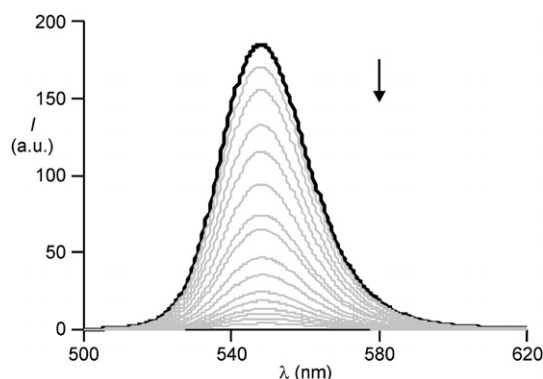


**Fig. 3** Emission spectra of QD-TOPO (0.08  $\mu\text{M}$ ,  $\text{CHCl}_3$ ,  $\lambda_{\text{EX}} = 400 \text{ nm}$ ) before (thick line) and after (thin lines) the addition of increasing amounts (0–1.5  $\mu\text{M}$ ) of **1·2Cl**.

### Luminescence quenching

The emission spectrum (Fig. 3, thick line) of a dispersion of QD-TOPO in  $\text{CHCl}_3$  shows an intense band centered at 547 nm with a luminescence quantum yield of 0.38 and an average luminescence lifetime of 16 ns. This band decreases in intensity (Fig. 3, thin lines) with the addition of increasing amounts of either **1·2Cl** or **1·2PF<sub>6</sub>** or even **2·2PF<sub>6</sub>**. However, the presence of either **1<sup>2+</sup>** or **2<sup>2+</sup>** has negligible influence on the absorption spectrum of QD-TOPO (Fig. 4).

In all instances, the concentration of the bipyridinium dication has negligible influence on the average luminescence lifetime (*a* in Fig. 5), but affects drastically the luminescence intensity (*b* in Fig. 5). These observations are consistent with static quenching and demonstrate that the luminescent nanoparticles and the dicationic quencher associate in the ground state. Interestingly, DLS measurements showed that the addition of a stoichiometric amount of **1·2Cl** to QD-TOPO causes an increase of the mean hydrodynamic diameter from  $9 \pm 1$  to  $12 \pm 2 \text{ nm}$ . This result is in agreement with the ground-state association of QD-TOPO with **1<sup>2+</sup>** and can be ascribed to an increase in the thickness of the organic shell, originating from the presence of the positively charged guest, its counteranions and, probably, additional solvent molecules. The association constants (*K*) and quenching

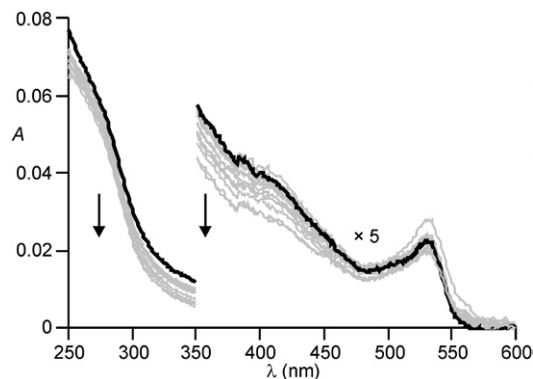


**Fig. 4** Absorption spectra of QD-TOPO (0.08  $\mu\text{M}$ ,  $\text{CHCl}_3$ ) before (thick line) and after (thin lines) the addition of increasing amounts (0–1.5  $\mu\text{M}$ ) of **1·2Cl**. The small absorbance decrease can be ascribed to dilution effects.

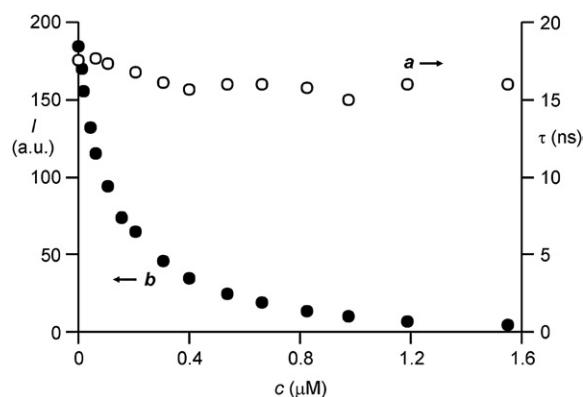


**Fig. 5** Plots of the average luminescence lifetime (*a*, right scale) and luminescence intensity (*b*, left scale) of QD-TOPO (0.08  $\mu\text{M}$ ,  $\text{CHCl}_3$ ,  $\lambda_{\text{EX}} = 400 \text{ nm}$ ) against the concentration of **1·2Cl**.

**Table 1** Association constants (*K*) for the complexes formed between QD-TOPO and the dicationic quenchers in  $\text{CHCl}_3$  and the corresponding quenching rate constants (*k<sub>q</sub>*)

	<i>K</i> / <i>M</i> <sup>-1</sup>	<i>k<sub>q</sub></i> / <i>s</i> <sup>-1</sup>
<b>1·2Cl</b>	$(1.1 \pm 0.1) \times 10^7$	$2.2 \times 10^9$
<b>1·2PF<sub>6</sub></b>	$(3.2 \pm 0.3) \times 10^5$	$1.7 \times 10^9$
<b>2·2PF<sub>6</sub></b>	$(1.7 \pm 0.2) \times 10^5$	$2.7 \times 10^8$

rate constants (*k<sub>q</sub>*) are listed in Table 1 and have been determined from the analysis of the Stern–Volmer plots.¶

A comparison of the data in Table 1 indicates that *K* increases by two orders of magnitude with the transition from hexafluorophosphate to chloride counterions and by *ca.* 50% with the elongation of the alkyl substituents from octyl to decyl chains. The former observation can be ascribed to a stronger solvophobic effect experienced by **1·2Cl** compared to **1·2PF<sub>6</sub>**, as reflected by the solubilities of these salts in chloroform. In contrast, the type of counterion of the quencher has little effect on the quenching rate constant, which however drops by one order of magnitude upon replacing the decyl side chains with octyl ones. In agreement with literature data,<sup>28</sup> electron transfer from the excited nanoparticles to either **1<sup>2+</sup>** or **2<sup>2+</sup>** is, presumably, responsible for quenching. Nonetheless, the characteristic spectroscopic signature of the radical cation of either **1<sup>2+</sup>** or **2<sup>2+</sup>** cannot be observed by nanosecond flash photolysis measurements, suggesting that back electron transfer occurs on a subnanosecond timescale. Since the redox properties of bipyridinium dications are nearly unaffected<sup>29</sup> by the type of alkyl substituent present on the nitrogen atoms, one can infer that the difference in the quenching rate constant between **1<sup>2+</sup>** and **2<sup>2+</sup>** is related to the fact that the former can approach closer to the QD surface compared to the latter.

The treatment of QD-TOPO with **3** results in the adsorption of the macrocyclic receptor on the surface of the nanoparticles.¶

¶ The analysis of the Stern–Volmer plots is discussed in the ESI.†

¶ The number of macrocyclic ligands adsorbed on each QD was not determined.

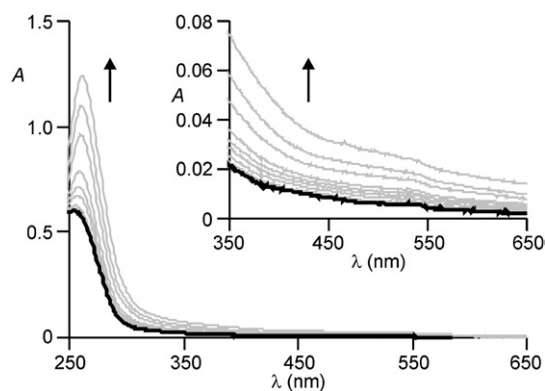


**Fig. 6** Absorption spectra of QD-3 (0.12  $\mu\text{M}$ ,  $\text{CHCl}_3$ ) before (thick line) and after (thin lines) the addition of increasing amounts (0–50  $\mu\text{M}$ ) of 1·2Cl. The inset shows a magnification of the region between 350 and 650 nm.

As a result, the luminescence quantum yield decreases by 30% with a bathochromic shift of 5 nm and the average luminescence lifetime drops to 9 ns. After the addition of increasing amounts of either 1·2Cl or 1·2PF<sub>6</sub> or even 2·2PF<sub>6</sub>, a broad and weak band extending up to 600 nm appears in the absorption spectrum (Fig. 6). Presumably, this absorption arises from charge-transfer interactions between the electron rich calixarene and the electron deficient dications.<sup>29</sup>

Once again, the luminescence intensity of the QDs decreases with the concentration of the bipyridinium dications, while the average luminescence lifetime remains essentially unaffected. This behavior is consistent with static quenching and confirms the formation of ground-state complexes between the luminescent nanoparticles and the dication quenchers. The corresponding  $K$  and  $k_q$  are listed in Table 2 and have been determined from the analysis of the Stern–Volmer plots. ¶

A comparison of the data in Table 2 indicates that  $K$  increases by one order of magnitude with the transition from hexafluorophosphate to chloride counterions and by ca. 50% with the elongation of the alkyl substituents from octyl to decyl chains. Interestingly, the nature of the ligands on the surface of the nanoparticles has a pronounced influence on  $K$ . Specifically, the bipyridinium complexes of QD–TOPO are significantly more stable than those of QD–3. This trend is in apparent contradiction with the known ability of calixarenes to encapsulate bipyridinium dications in nonpolar solvents with high association constants.<sup>29</sup> Presumably, the confinement of 3 on the surface of the inorganic nanoparticles hinders the insertion of either 1<sup>2+</sup> or 2<sup>2+</sup> into its cavity. Chloride anions may favor the association between QD–3 and 1<sup>2+</sup> because they can form hydrogen bonds with the ureidic units of 3.<sup>29</sup>

**Table 2** Association constants ( $K$ ) for the complexes formed between QD–3 and the dicationic quenchers in  $\text{CHCl}_3$  and the corresponding quenching rate constants ( $k_q$ )

	$K/\text{M}^{-1}$	$k_q/\text{s}^{-1}$
1·2Cl	$(1.0 \pm 0.1) \times 10^5$	$5.4 \times 10^8$
1·2PF <sub>6</sub>	$(2.4 \pm 0.4) \times 10^4$	$1.2 \times 10^8$
2·2PF <sub>6</sub>	$(1.0 \pm 0.1) \times 10^4$	$2.0 \times 10^8$

The  $k_q$  values are one order of magnitude smaller than those measured for QD–TOPO. These observations can be rationalized considering that the inclusion of 1<sup>2+</sup> or 2<sup>2+</sup> into 3 is expected to have two main consequences. First, their bipyridinium units are kept separated from the QD surface by the monolayer formed by the undecanethiol-derivatized calixarene; second, they become more difficult to reduce, thereby decreasing the driving force for the electron-transfer process.<sup>29</sup>

### Competitive binding

The calixarene 4 (Fig. 1) binds bipyridinium dications in nonpolar solvents with association constants of ca.  $10^6 \text{ M}^{-1}$ .<sup>29</sup> As a result, this macrocyclic receptor can compete with QD–TOPO and capture any of the three bipyridinium quenchers 1·2Cl, 1·2PF<sub>6</sub> or 2·2PF<sub>6</sub>. For example, the luminescence intensity of QD–TOPO ( $a$  in Fig. 7) is almost completely suppressed in the presence of ca. 19 equivalents of 1·2Cl ( $b$  in Fig. 7). However, the original luminescence intensity is fully restored after the addition of an excess of 4 ( $c$  in Fig. 7). Indeed, the supramolecular association of 4 and 1<sup>2+</sup> prevents the interaction of the latter with QD–TOPO and suppresses the photoinduced electron-transfer process. Consistently, this supramolecular event is transduced into a pronounced enhancement in luminescence. Thus, these operating principles can, in principle, be exploited to probe receptor–substrate interactions with luminescence measurements.

### Conclusions

We have prepared CdSe–ZnS core–shell quantum dots coated with either TOPO or calixarene 3, and investigated the interaction of these nanoparticles with two bipyridinium derivatives.

Our results demonstrate that bipyridinium dications associate with either QD–TOPO or QD–3 in the ground state with  $K$  ranging from  $10^4$  to  $10^7 \text{ M}^{-1}$  in  $\text{CHCl}_3$ . The counterions of the bipyridinium dications as well as the ligands on the surface of the QDs control the stability of the resulting complexes. The length of the aliphatic chains appended to the bipyridinium core has a minor influence on the binding event. In these supramolecular assemblies, the bipyridinium dications quench the luminescence of the nanoparticles with  $k_q$  ranging from  $10^8$  to

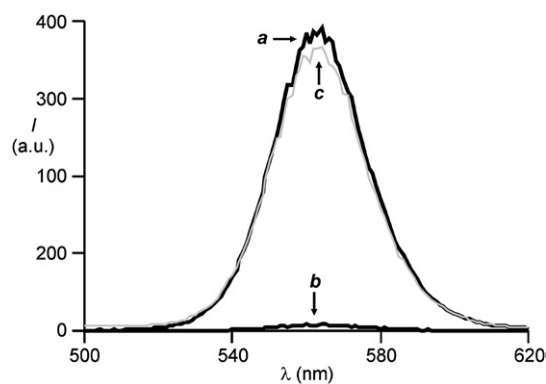


**Fig. 7** Emission spectra of QD–TOPO (0.43  $\mu\text{M}$ ,  $\text{CHCl}_3$ ,  $\lambda_{\text{Ex}} = 350 \text{ nm}$ ) before ( $a$ ) and after the sequential addition of 1·2Cl ( $b$ , 8.0  $\mu\text{M}$ ) and 4 ( $c$ , 160  $\mu\text{M}$ ).

$10^9 \text{ s}^{-1}$ , presumably by photoinduced electron transfer from the inorganic core. Interestingly, the transition from TOPO to **3** ligands has a depressive effect on the stability of the bipyridinium complexes and delays the quenching process significantly. In the presence of **4**, the bipyridinium quenchers desorb from the surface of QD–TOPO and associate with the calixarene instead. As a result, the original luminescence intensity of the nanoparticles is restored. Thus, the supramolecular association of the quencher with a complementary receptor can be transduced into a luminescence enhancement with these operating principles.

## Experimental

### Materials and methods

**Chemicals.** QD–TOPO, **1**<sup>+</sup>, **2**<sup>+</sup>, **4**, **5** and toluene-4-sulfonic acid undec-10-enyl ester were synthesized according to literature procedures.<sup>21,22,24–26</sup> All reactions were carried out under  $\text{N}_2$  and all solvents were freshly distilled under  $\text{N}_2$  prior to use. All other chemicals were reagent grade quality, obtained from commercial supplies and used without further purification.

**Purification and characterization.** Thin-layer chromatography was performed on aluminium sheets coated with silica gel 60F (Merck 5554). Column chromatography was carried out by using silica gel (ICN 4663, 63–200 mesh). <sup>1</sup>H NMR spectra were recorded at 300 MHz. <sup>13</sup>C NMR spectra were recorded at 75 MHz. Mass spectra were recorded in the ESI mode.

**Particle size distribution.** The nanoparticle size distribution was determined by DLS with a Malvern Nano ZS instrument equipped with a 633 nm laser diode. Measurements were carried out at 0 °C in air-equilibrated  $\text{CHCl}_3$  solutions placed in 1 cm quartz cuvettes. The samples were filtered twice through 0.1  $\mu\text{m}$  PTFE membrane filters prior to the measurements. The resulting size is the average of at least 20 independent experiments, and the standard deviation is taken as the experimental error.

**Photophysical experiments.** Absorption spectra were recorded with a Perkin Elmer  $\lambda$ 40 spectrophotometer in air equilibrated  $\text{CHCl}_3$  (Merck Uvasol™) solutions at room temperature (*ca.* 25 °C), contained in 1 cm spectrofluorimetric quartz cells. Luminescence spectra were recorded with either an Edinburgh Instruments FLS920 or a Varian Cary Eclipse, exciting the sample at either 400 or 350 nm respectively. Luminescence lifetimes were determined with the Edinburgh Instruments FLS920, exciting the sample at 400 nm. The experimental errors are  $\pm 1 \text{ nm}$  for the wavelengths and  $\pm 10\%$  for the luminescence intensities and lifetimes.

The luminescence decay of the QDs, both alone and in the presence of the quencher, is not monoexponential and could be fitted by a double exponential function. Mean lifetime values, obtained from a weighted average of the two individual lifetimes on the basis of their relative contribution to the decay, were taken as an indication of the QDs excited-state lifetime.<sup>30</sup> The titration of the QDs with the quencher was performed by adding small aliquots (typically 5  $\mu\text{l}$ ) of a 10  $\mu\text{M}$  solution of the quencher to 2.5 mL of a dilute (<0.2  $\mu\text{M}$ ) solution of the QDs by using a microsyringe.

### Synthesis of 6

Calix[6]arene **5** (1.5 g, 1.5 mmol) and toluene-4-sulfonic acid undec-10-enyl ester (1.7 g, 5.4 mmol) were dissolved in 500 ml of acetonitrile.  $\text{K}_2\text{CO}_3$  (0.8 g, 5.4 mmol) was added and the resulting heterogeneous mixture was refluxed for 7 days. After this period HCl (300 ml 10% in water) and ethyl acetate (100 ml) were added. The organic phase was separated, dried on  $\text{Na}_2\text{SO}_4$  and concentrated under reduced pressure. The crude product was purified by column chromatography (eluent: hexane–ethyl acetate = 95 : 5) obtaining calix[6]arene **6** as a yellowish solid (yield 69%). <sup>1</sup>H NMR (300 MHz,  $\text{CDCl}_3$ )  $\delta$  7.67 (bs, 6 H), 7.21 (bs, 6 H), 5.9–5.7 (m, 3 H), 5.0–4.9 (m, 6 H), 4.6–4.1 (m, 6 H), 3.83 (bs, 6 H), 3.7–3.4 (m, 6 H), 2.86 (s, 9 H), 2.1–2.0 (m, 6 H), 1.85 (bs, 6 H), 1.6–1.0 (m, 53 H). <sup>13</sup>C NMR (75 MHz,  $\text{CDCl}_3$ ): 146.8, 143.6, 139.1, 127.8, 127.3, 123.1, 114.1, 77.4, 73.9, 59.9, 34.2, 33.7, 31.4, 31.2, 30.9, 30.5, 30.2, 29.4, 29.2, 29.0, 28.8, 26.0. Mp 138–140 °C. ESIMS: 1461.68 [ $\text{M} + \text{Na}^+$ ].

### Synthesis of 7

Calix[6]arene **6** (1.3 g, 0.9 mmol) and thioacetic acid (0.2 g, 2.8 mmol) were dissolved in 100 ml of dry toluene. AIBN was added (catalytic amount) and the mixture refluxed for 12 h. After this period distilled water (300 ml) was added. The organic phase collected and concentrated under reduced pressure. Pure **7** was obtained by column chromatography (eluent: hexane–THF = 9 : 1) as a yellowish solid (yield 83%). <sup>1</sup>H NMR (300 MHz,  $\text{CDCl}_3$ )  $\delta$  7.68 (bs, 6 H), 7.23 (bs, 6 H), 4.6–4.1 (m, 6 H), 3.83 (bs, 6 H), 3.7–3.4 (m, 6 H), 2.9–2.8 (m, 15 H), 2.3 (s, 9 H), 1.85 (bs, 6 H), 1.7–1.0 (m, 53 H). <sup>13</sup>C NMR (75 MHz,  $\text{CDCl}_3$ ): 195.8, 159.8; 154.2; 146.7; 143.5, 135.7, 132.1, 129.7, 127.8, 127.3, 123.1, 73.9, 59.8, 34.2, 31.4, 30.9, 30.5, 30.2, 29.4, 29.0, 28.7, 26.8, 26.0, 23.3. Mp 146–148 °C. ESIMS: 1686.66 [ $\text{M} + \text{Na}^+$ ].

### Synthesis of 8

Calix[6]arene **7** (1 g, 0.6 mmol) was dissolved in THF (50 ml) and HCl (50 ml 10% in water) and the resulting homogeneous mixture refluxed for 3 days. After this period ethyl acetate (20 ml) was added, the organic phase separated, dried on  $\text{Na}_2\text{SO}_4$  and concentrated under reduced pressure to obtain compound **8**, which was used for the next reaction without any other purification.

### Synthesis of 9

Calix[6]arene **8** (0.6 g, 0.4 mmol), trityl chloride (0.5 g, 1.8 mmol) and triethylamine (0.2 g, 2 mmol) were dissolved in acetonitrile (50 ml) and refluxed for 12 h. After this period the solvent was removed and the residue dissolved in ethyl acetate (100 ml). The organic phase was washed twice with HCl (100 ml 10% in water), dried on  $\text{Na}_2\text{SO}_4$  and concentrated under reduced pressure. Compound **9** was purified by column chromatography (eluent: hexane–ethyl acetate = 9 : 1) as a yellowish solid (yield 77%). <sup>1</sup>H NMR (300 MHz,  $\text{CDCl}_3$ )  $\delta$  7.67 (bs, 6 H), 7.6–7.1 (m, 51 H), 4.6–4.1 (m, 6 H), 3.81 (bs, 6 H), 3.7–3.4 (bs, 6 H), 2.85 (s, 9 H), 2.12 (t, 6 H,  $J = 7.3 \text{ Hz}$ ), 1.83 (bs, 6 H), 1.8–1.0

(m, 53 H).  $^{13}\text{C}$  NMR (75 MHz,  $\text{CDCl}_3$ ): 146.8, 145.1, 132.1, 129.9, 129.6, 129.5, 129.3, 128.9, 128.7, 128.3, 128.2, 127.9, 127.7, 127.6, 127.4, 127.3, 127.2, 126.6, 126.4, 126.3, 123.1, 115.3, 73.9, 66.33, 34.2, 32.0, 31.4, 30.2, 29.7, 29.5, 29.4, 29.2, 29.0, 28.6, 25.0. Mp 100–103 °C. ESIMS: 2288.66 [ $\text{M} + \text{Na}^+$ ].

### Synthesis of 10

In a 250 ml two neck round bottom flask calix[6]arene **9** (0.58 g, 0.26 mmol) was suspended in *n*-butanol (150 ml). Pd on activated charcoal (catalytic amount) was added under nitrogen. The mixture was stirred for a few minutes and then hydrazine monohydrate (0.64 g, 13 mmol) was added. The resulting heterogeneous mixture was refluxed for 12 h. The crude of the reaction was cooled to room temperature and the Pd/C removed by filtration on Celite maintaining the equipment under  $\text{N}_2$  atmosphere. The solvent was removed under reduced pressure and the triamine calix[6]arene **10** was used for the next reaction without any other purification.

### Synthesis of 11

Calix[6]arene **10** (0.55 g, 0.25 mmol) and phenylisocyanate (0.15 g, 1.26 mmol) were dissolved in dry  $\text{CH}_2\text{Cl}_2$  (100 ml) and stirred at room temperature for 4 h. The organic solvent was removed under reduced pressure and the crude compound **11** was triturated in methanol to obtain calix[6]arene as a pale yellow solid (yield 84%).  $^1\text{H}$  NMR (300 MHz,  $\text{CDCl}_3$ )  $\delta$  7.7–6.8 (m, 72 H), 6.30 (s, 6 H), 4.38 (d, 6 H,  $J = 15.1$  Hz), 3.89 (bt, 6 H), 3.54 (d, 6 H,  $J = 15.4$  Hz), 2.82 (bs, 9 H), 2.13 (t, 6 H,  $J = 7.2$  Hz), 1.87 (bs, 6 H), 1.55 (bs, 6 H), 1.5–1.0 (m, 47 H).  $^{13}\text{C}$  NMR (75 MHz,  $\text{CDCl}_3$ ): 154.9, 154.4, 152.0, 146.8, 145.0, 138.0, 135.5, 132.9, 132.3, 129.5, 128.8, 128.2, 127.8, 127.7, 127.2, 126.4, 123.4, 122.5, 120.5, 73.1, 66.3, 60.2, 34.2, 32.0, 31.5, 30.9, 30.5, 29.5, 29.3, 29.1, 28.9, 28.5, 26.2. Mp 128–130 °C. ESIMS: 2557.23 [ $\text{M} + \text{Na}^+$ ].

### Synthesis of 3

Calix[6]arene **11** (0.05 g, 0.02 mmol) was dissolved in  $\text{CH}_2\text{Cl}_2$  (20 ml) and TFA (10 ml).  $\text{NaBH}_3\text{CN}$  (0.006 g, 0.1 mmol) was added and the mixture stirred at room temperature for 3 h. Water (30 ml) was added and the organic phase collected, dried on  $\text{Na}_2\text{SO}_4$  and concentrated under reduced pressure. The crude product was triturated in methanol to obtain calix[6]arene **3** as a pale yellow solid (yield 86%).  $^1\text{H}$  NMR (300 MHz,  $\text{CDCl}_3$ )  $\delta$  7.4–6.8 (m, 27 H), 6.27 (s, 6 H), 4.38 (d, 6 H,  $J = 15.4$  Hz), 3.90 (t, 6 H,  $J = 6.0$  Hz), 3.55 (d, 6 H,  $J = 15.6$  Hz), 2.82 (bs, 9 H), 2.51 (q, 6 H,  $J = 7.2$  Hz), 1.88 (t, 6 H,  $J = 6.8$  Hz), 1.8–1.0 (m, 53 H).  $^{13}\text{C}$  NMR (75 MHz,  $\text{CDCl}_3$ ): 154.9, 154.5, 152.3, 146.7, 138.2, 135.7, 133.0, 132.3, 129.4, 129.3, 128.8, 128.7, 128.20, 127.6, 126.2, 123.4, 123.1, 120.5, 73.0, 60.2, 34.1, 34.0, 31.8, 31.5, 31.0, 30.5, 29.6, 29.5, 29.4, 29.3, 29.2, 29.0, 28.8, 28.3, 26.2, 24.6. Mp 137–142 °C. ESIMS: 1830.6 [ $\text{M} + \text{Na}^+$ ].

### Synthesis of QD-3

A dispersion of QD-TOPO (10 mg) and **3** (40 mg) in  $\text{CHCl}_3$  (20 ml) was heated under reflux for 24 h. After cooling to

ambient temperature, the solvent was distilled off under reduced pressure. The residue was dissolved in  $\text{CHCl}_3$  (2 ml) and diluted with MeOH (30 ml). The resulting precipitate was filtered off after centrifugation. This procedure was repeated three more times to afford QD-3 (8 mg) as a reddish powder.

### References

- 1 M. G. Bawendi, M. L. Steigerwald and L. E. Brus, *Annu. Rev. Phys. Chem.*, 1990, **41**, 477–496.
- 2 A. P. Alivisatos, *Science*, 1996, **271**, 933–937.
- 3 Al. L. Efros and L. Rosen, *Annu. Rev. Mater. Sci.*, 2000, **30**, 475–521.
- 4 A. D. Yoffe, *Adv. Phys.*, 2001, **50**, 1–208.
- 5 C. Burda, X. B. Chen, R. Narayana and M. A. El-Sayed, *Chem. Rev.*, 2005, **105**, 1025–1102.
- 6 C. M. Niemeyer, *Angew. Chem., Int. Ed.*, 2003, **42**, 5796–5800.
- 7 I. Willner and E. Katz, *Angew. Chem., Int. Ed.*, 2004, **43**, 6042–6108.
- 8 A. P. Alivisatos, *Nat. Biotechnol.*, 2004, **22**, 47–52.
- 9 N. L. Rosi and C. A. Mirkin, *Chem. Rev.*, 2005, **105**, 1547–1562.
- 10 X. Gao, L. Yang, J. A. Petros, F. F. Marshall, J. W. Simons and S. Nie, *Curr. Opin. Biotechnol.*, 2005, **16**, 63–72.
- 11 I. G. Medintz, H. T. Uyeda, E. R. Goldam and H. Mattoussi, *Nat. Mater.*, 2005, **4**, 435–446.
- 12 X. Michalet, F. F. Pinaud, L. A. Bentolila, J. M. Tsay, S. Doose, J. J. Li, G. Sundaresan, A. M. Wu, S. S. Gambhir and S. Weiss, *Science*, 2005, **307**, 538–544.
- 13 R. C. Somers, M. G. Bawendi and D. G. Nocera, *Chem. Soc. Rev.*, 2007, **36**, 579–591.
- 14 F. M. Raymo and I. Yildiz, *Phys. Chem. Chem. Phys.*, 2007, **9**, 2036–2043.
- 15 (a) M. G. Sandros, D. Gao and D. E. Benson, *J. Am. Chem. Soc.*, 2005, **127**, 12198–12199; (b) B. P. Aryal and D. E. Benson, *J. Am. Chem. Soc.*, 2006, **128**, 15986–15987.
- 16 K. Palaniappan, C. Xue, G. Arumugam, S. A. Hackney and J. Liu, *Chem. Mater.*, 2006, **18**, 1275–1280.
- 17 R. Gill, R. Freeman, J.-P. Xu, I. Willner, S. Winograd, I. Shweky and U. Banin, *J. Am. Chem. Soc.*, 2006, **128**, 15376–15377.
- 18 (a) I. Yildiz and F. M. Raymo, *J. Mater. Chem.*, 2006, **16**, 1118–1120; (b) M. Tomasulo, I. Yildiz and F. M. Raymo, *J. Phys. Chem. B*, 2006, **110**, 3853–3855; (c) M. Tomasulo, I. Yildiz, S. L. Kaanumalle and F. M. Raymo, *Langmuir*, 2006, **22**, 10284–10290; (d) I. Yildiz, M. Tomasulo and F. M. Raymo, *Proc. Natl. Acad. Sci. U. S. A.*, 2006, **103**, 11457–11460.
- 19 V. Maruel, M. Laferrrière, P. Billone, R. Godin and J. C. Sciano, *J. Phys. Chem. B*, 2006, **110**, 16353–16358.
- 20 S. J. Clarke, C. A. Hollmann, Z. Zhang, D. Suffern, S. E. Bradforth, N. M. Dimitrijevic, W. G. Minarik and J. L. Nadeau, *Nat. Mater.*, 2006, **5**, 409–417.
- 21 B. O. Dabbousi, J. Rodriguez-Viejo, F. V. Mikulec, J. R. Heine, H. Mattoussi, R. Ober, K. F. Jensen and M. G. Bawendi, *J. Phys. Chem. B*, 1997, **101**, 9463–9475.
- 22 Z. A. Peng and X. Peng, *J. Am. Chem. Soc.*, 2001, **123**, 183–184.
- 23 J. M. Tsay, S. Doose and S. Weiss, *J. Am. Chem. Soc.*, 2006, **128**, 1639–1647.
- 24 A. Arduini, R. Ferdani, A. Pochini, A. Secchi and F. Ugozzoli, *Angew. Chem., Int. Ed.*, 2000, **39**, 3453–3456.
- 25 R. J. Alvarado, J. Mukherjee, E. J. Pacsial, D. Alexander and F. M. Raymo, *J. Phys. Chem. B*, 2005, **109**, 6164–6173.
- 26 J. J. Gonzales, R. Ferdani, E. Albertini, J. M. Blasco, A. Arduini, A. Pochini, P. Prados and J. De Mendoza, *Chem.–Eur. J.*, 2000, **6**, 73–80.
- 27 R. Métivier, I. Leray, B. Lebeau and B. Valeur, *J. Mater. Chem.*, 2005, **15**, 2965–2973.
- 28 (a) S. Logunov, T. Green, S. Marguet and M. A. El-Sayed, *J. Phys. Chem. A*, 1998, **102**, 5652–5658; (b) C. Burda, T. C. Green, S. Link and M. A. El-Sayed, *J. Phys. Chem. B*, 1999, **103**, 1783–1788.
- 29 A. Credi, S. Dumas, S. Silvi, M. Venturi, A. Arduini, A. Pochini and A. Secchi, *J. Org. Chem.*, 2004, **69**, 5881–5887.
- 30 J. R. Lakowicz, *Principles of Fluorescence Spectroscopy*, Springer, New York, 2006.